

1 **APWP-online.org: a global reference database and open-source tools for**
2 **calculating apparent polar wander paths and relative paleomagnetic**
3 **displacements**

4
5 **Bram Vaes^{1*}, Douwe J.J. van Hinsbergen¹ & Joren Paridaens²**

6 ¹Department of Earth Sciences, Utrecht University, Utrecht, The Netherlands

7 ²de online, Utrecht, The Netherlands

8 * Corresponding author (e-mail: b.vaes@uu.nl)

9
10 **Abstract**

11 Paleomagnetism provides a quantitative tool for estimating paleogeographic displacements of rock
12 units relative to the Earth's spin axis and is widely used to determine relative tectonic displacements
13 (vertical-axis rotations and paleolatitudinal motions). These relative displacements are commonly
14 determined by comparing a study-mean paleomagnetic pole with a reference pole provided by an
15 apparent polar wander path (APWP), even though these poles are calculated by averaging
16 paleomagnetic data from different hierarchical levels. This conventional approach was recently
17 shown to strongly overestimate the resolution at which paleomagnetic displacements can be
18 determined. This problem was recently overcome by comparing paleomagnetic poles computed at the
19 same hierarchical level, whereby the uncertainty of the reference pole is weighed against the number
20 of datapoints underlying the study-mean pole. To enable the application of this approach, a new global
21 APWP was calculated for the last 320 Ma from (simulated) site-level paleomagnetic data. Applying
22 this method requires a computationally more intensive procedure, however. Here, we therefore
23 present the online, open-source environment *APWP-online.org* that provides user-friendly tools to
24 determine relative paleomagnetic displacements and to compute APWPs from site-level
25 paleomagnetic data. In addition, the website hosts the curated paleomagnetic database used to
26 compute the most recent global APWP and includes an interface for adding new high-quality
27 paleomagnetic data that may be used for future iterations of the global APWP. We illustrate how the
28 tools can be used through two case studies: the vertical-axis rotation history of the Japanese Islands
29 and the paleolatitudinal motion of the intra-oceanic Olyutorsky arc exposed on Kamchatka.

30
31 **Key words:** paleomagnetism, apparent polar wander path, paleogeography, paleomagnetic pole,
32 reference frame, paleolatitude, plate reconstruction

33
34 **This paper is a non-peer reviewed manuscript submitted to EarthArXiv. The manuscript**
35 **has been submitted for peer review to *Tektonika*.**

36 **1. Introduction**

37 Paleomagnetic data – obtained from measurements of the remanence magnetization recorded in
38 rocks – provide a quantitative tool for studying the paleogeographic history and interpreting the
39 relative and absolute motions of tectonic plates and smaller, fault-bounded terranes (e.g., Cox and
40 Hart, 1986; Butler, 1992). One of the main tectonic applications of paleomagnetism is the
41 identification and quantification of two types of relative displacements: vertical-axis rotations and
42 paleolatitudinal motions. To quantify such displacements, paleomagnetists typically compare a study-
43 mean paleomagnetic direction or pole from a studied geological record, e.g., a fault-bounded block –
44 with a reference direction or pole that represents a nearby stable tectonic plate, often provided by an
45 apparent polar wander path (APWP) (e.g., Demarest, 1983; Coe et al., 1985; Butler, 1992).
46 Conventional APWPs, computed by averaging a collection of study-mean paleopoles whose mean age
47 fall into a fixed time window, provide reference poles with an A_{95} cone of confidence that allow a
48 straightforward comparison with a study-mean pole and its A_{95} , computed instead by averaging a
49 collection ‘spot readings’ of the past geomagnetic field. Statistical differences between a study-mean
50 pole and a reference pole (from an APWP) are routinely interpreted as evidence for relative tectonic
51 motions. However, Rowley (2019) recently showed that more than half of the study-mean poles that
52 were used to compute the widely used global APWP of Torsvik et al. (2012) are statistically distinct
53 (or ‘discordant’) from the reference pole position to which they contributed. This shows that the
54 conventional approach to determine paleomagnetic displacements cannot reliably demonstrate
55 tectonically meaningful displacements (Rowley, 2019).

56 Vaes et al. (2022) showed that the underlying problem is that conventional APWPs have been
57 computed from paleomagnetic data at a different hierarchical level than study-mean poles: the
58 reference direction or pole is computed from site-means, whereas the study-level direction or pole is
59 instead computed from a collection of spot readings (i.e., paleomagnetic sites). These authors
60 demonstrated that an alternative approach computing APWPs on site-level paleomagnetic data,
61 rather than pole-level data, offers a solution to this problem. They showed that when the uncertainty
62 of the reference pole is weighted against the number of site-level datapoints in the study-mean pole,
63 a statistical difference can be interpreted as geologically meaningful. In this approach, the reference
64 pole position and its uncertainty are determined from a large number (>1000) of synthetic reference
65 poles that are calculated from the same number of sites in the studied paleomagnetic dataset. The
66 resolution at which a statistical difference, and thus a tectonic displacement, may be determined is
67 thus directly controlled by the size of the studied dataset. In contrast to the conventional approach,
68 the methodology developed by Vaes et al. (2022) also weights the spatial and temporal uncertainties
69 in the underlying paleomagnetic data in the computation of the reference pole and its confidence
70 region. Building on this study, Vaes et al. (2023) presented a global APWP (combining all
71 paleomagnetic data from stable plate interiors whose relative motions are well-constrained, e.g., by
72 ocean basin reconstructions (Besse & Courtillot, 2002; Torsvik et al., 2008, 2012) calculated from

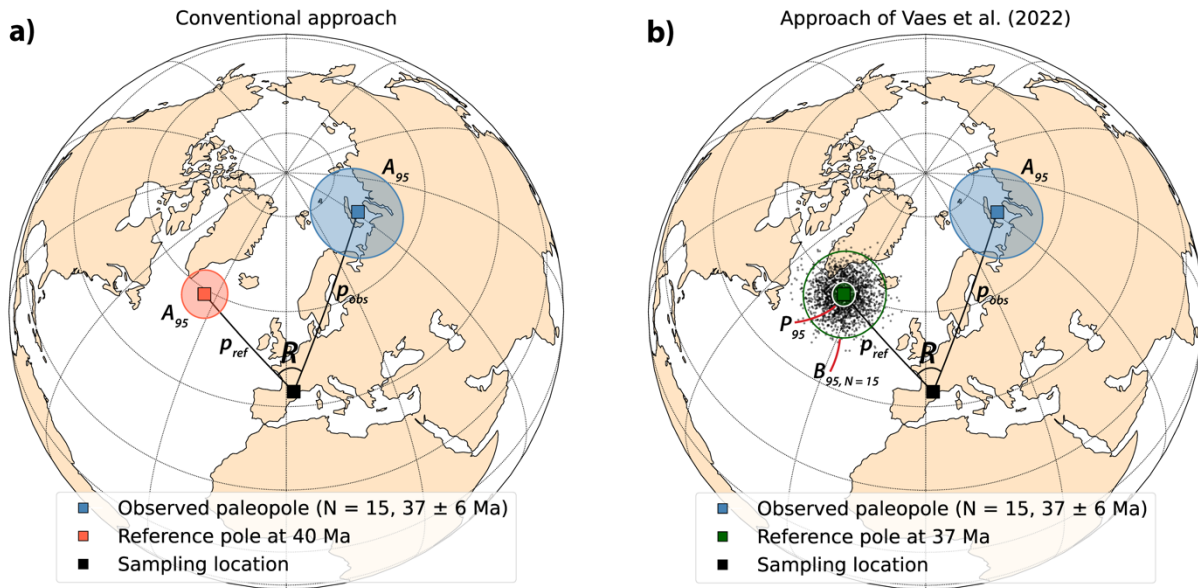


73

Fig. 1. Overview of the homepage of APWP-online.org.

74 parametrically re-sampled site-level data. This provides a new reference frame that allows the
75 determination of paleomagnetic displacements by comparing paleomagnetic data on the same
76 hierarchical level. However, this new approach requires a bootstrapped approach to determine the
77 reference pole and its uncertainty, which is computationally more complex than the conventional
78 approach.

79 Here, we present the online and open-source environment *APWP-online.org* that provides a set
80 of tools to compute relative paleomagnetic displacements and custom APWPs using the approaches
81 presented by Vaes et al. (2022, 2023). This web application also includes a portal providing access to
82 the curated paleomagnetic database that was used to compute the global APWP of Vaes et al. (2023),
83 together with an interface where paleomagnetists can request the addition of new high-quality
84 paleomagnetic data, or revision of age constraints, that may be used for future updates of the global
85 APWP. We illustrate how these two portals may contribute to solving tectonic problems by applying
86 them to two case-studies: the timing and magnitude of the Neogene rotations of the Japanese islands
87 and the paleolatitudinal evolution of the Late Cretaceous-Paleogene intra-oceanic Olyutorsky arc
88 (Kamchatka).



89

90 **Fig. 2.** Comparison between the conventional approach and the recently developed approach by Vaes
 91 et al. (2022) for the determination of relative tectonic displacements.

92

93 2. Tools

94 2.1. APWP tool

95 The APWP tool allows users to compute an APWP based on site-level paleomagnetic data using the
 96 approach of Vaes et al. (2023). The APWP is calculated from virtual geomagnetic poles (VGPs) that are
 97 parametrically re-sampled from a custom-provided collection of paleopoles, rather than from those
 98 paleopoles itself. To compute the APWP, the user first needs to specify the age range for the APWP,
 99 size of the time window and the time step at which the reference poles of the APWP are computed
 100 (Fig. 3). This tool can be used to construct an APWP for any plate or terrane regardless of the age of
 101 rocks from which the data are derived, as long as the input data are provided in the coordinate system
 102 of the same plate or terrane. The website includes a tool to rotate paleopoles into the coordinates of a
 103 different plate based on user-provided relative Euler rotation poles (Fig. 3). Prior to initializing the
 104 APWP tool, the user can also choose the number of iterations used for the computation of the path and
 105 the estimation of its 95% confidence region (the P_{95} of Vaes et al. (2023), see Fig. 2b), like the Relative
 106 Paleomagnetic Displacement tool described in the next section. It is important to note that a very large
 107 number (1000s) of iterations will significantly slow down the computation time.

108 For each iteration of the APWP computation, the re-sampled VGPs are assigned a random age
 109 within the age uncertainty range of the pole from which they are generated. Next, a sliding window
 110 is applied to the VGPs, computing an estimate of the reference pole for each time step by averaging the
 111 *pseudo*-VGPs that fall within the time window centered on that age. The final APWP is computed as
 112 the average of the simulated reference poles per time window, with the P_{95} confidence region defined
 113 as the circle that includes 95% of those simulated reference poles. For a more detailed explanation of
 114 the workflow, we refer the reader to section 3 of Vaes et al. (2023).

APWP Tool

This tool allows you to compute an APWP based on site-level paleomagnetic data using the approach of Vaes et al. (2023).

Show more ▾

LOAD INPUT FILES ☺ data will be stored and processed locally on your own machine.

+

Add your dataset
xlsx or csv

Load in demo data

or download the example input file

NEJ
NEJ.OSM (3.2 MB)
37 poles

This set is active

SWJ
SWJ.OSM (3.2 MB)
37 poles

Use this set

CALCULATIONS ☺ calculations will done locally on your own machine.

Window length (Ma) Time step (Ma)

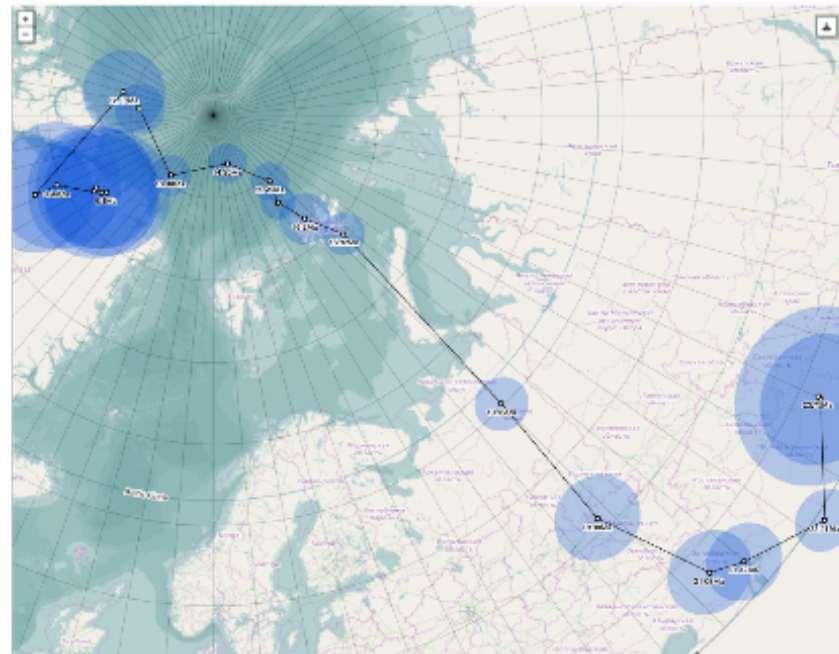
Minimum age (Ma) Maximum age (Ma)

Number of iterations

Calculate APWP



CALCULATED APWP



115
116 **Fig. 3.** Overview of the APWP tool.

117
118 The tool also facilitates the straightforward reproduction of the global APWP of Vaes et al.
119 (2023) and can be directly applied to the reference database that is available under the Reference

120 database portal (see section 5). Moreover, it allows users to compute custom APWPs from a filtered
121 set of paleopoles included in that database. For instance, one may calculate an APWP solely based on
122 the data derived from a chosen plate, e.g., South America, using a different window size and time step
123 as used by Vaes et al. (2023). Researchers may also apply this tool to evaluate the effect of a new
124 paleomagnetic dataset on the global APWP.

125

126 **2.2. Relative Paleomagnetic Displacement (RPD) tool**

127 The second tool of APWP-online.org (Fig. 4) allows the determination of a relative paleomagnetic
128 displacement (RPD) using the comparison metric that was introduced by Vaes et al. (2022). Central to
129 this approach is the comparison between an observed paleopole and a reference pole in which the
130 number of paleomagnetic sites used to compute the paleopole is taken into consideration. The 95%
131 confidence region of the reference pole (the B_{95}) is estimated as if it had been derived from the same
132 number of sites as the observed paleopole (N_s) (see Fig. 2). To determine the reference and the B_{95} we
133 use the parametric bootstrap approach described by Vaes et al. (2022). For each run the tool computes
134 a single estimate for the position of the reference pole – a *pseudopole* – using two steps. First, VGPs
135 are generated by parametric re-sampling of all paleopoles included in the reference database, whose
136 age uncertainty range overlaps with that of the studied dataset. For each paleopole, VGPs are re-
137 sampled from a Fisher (1953) distribution centered on the paleopole position and defined by the
138 reported precision parameter K , whereby the number of VGPs corresponds to the number of sites
139 used by the original authors to compute that pole. Next, a pseudopole is computed by averaging N_s
140 randomly drawn VGPs whose age falls within the age uncertainty range of the studied dataset. A
141 distribution of pseudopoles is then obtained after repeating this procedure hundreds to thousands of
142 times (as specified by the user, see Fig. 4). Vaes et al. (2022) defined the B_{95} as the radius of the circle
143 about the principal vector of the pseudopoles that includes 95% of those pseudopoles (Fig. 2). The
144 size of the B_{95} is directly dependent on the N_s and becomes larger with decreasing N_s , such that the
145 resolution of the statistics comparison is adjusted to the amount of information contained in the
146 studied dataset. This way, the reference pole and the B_{95} simply show the uncertainty in the position
147 of the reference pole, predicting where it could be located if it would have been calculated from the
148 same number of VGPs as included in the studied dataset.

149 The reference data used to compute the relative paleomagnetic displacements can be chosen
150 by the user (Fig. 4). To determine the displacements of a collection of paleopoles relative to a large
151 tectonic plate (North America, South America, Eurasia, Iberia, Africa, India, Antarctica, Australia,
152 Pacific), the reference pole position is computed from the database underlying the global APWP of
153 Vaes et al. (2023). To this end, all re-sampled VGPs are rotated to the chosen reference plate using
154 pre-calculated Euler rotation poles that are derived from the global plate circuit used by Vaes et al.
155 (2023). For each input paleopole, a default age range of 10 Ma around the mean age of the pole is used.
156 This age range can be modified by the user (Fig. 4), e.g., to exactly match the age range of the observed

RPD Tool

The relative paleomagnetic displacement (RPD) tool allows the determination of displacements using the comparison metric that was introduced by Vaas et al. (2022).

Show more ▾

LOAD INPUT FILES data will be stored and processed locally on your own machine.

Add your dataset
xlsx or csv

Load in demo data

or download the example input file

NEJ
NEJ.csv (12 #)
37 poles

This set is active

SWJ
SWJ.csv (12 #)
37 poles

Use this set

CALCULATIONS calculations will done locally on your own machine.

Input dataset

Number of iterations Time window (Ma)

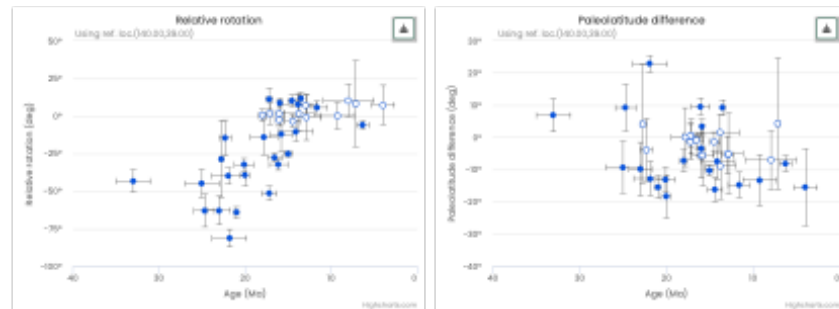
Reference location Longitude Latitude

Choose reference Reference plate



Calculate displacements

CALCULATED ROTATION AND DISPLACEMENT



APWP-ONLINE
Home
APWP Tool
RPD Tool
Reference database
About

CONTACT
info@apwp-online.org Department of Earth Sciences
Utrecht University,
Van der Hoeven Building A,
Princetonlaan 8A,
3584 CB Utrecht, Netherlands

SUPPORTED BY

157

158 **Fig. 4.** Overview of the relative paleomagnetic displacement (RPD) tool.

159 paleopole. With age uncertainties of a few to ten million years, this is not likely to affect the result, but
 160 this can be evaluated for each individual case by the user.

161 The user may also upload a custom reference database to the RPD tool, allowing the
 162 determination of RPDs using reference poles computed from this database. This can be done by
 163 choosing the right uploaded file under ‘Choose reference’ (Fig. 4). It is important to note that the
 164 reference data should be provided using the template input file (see section 2.3), hence consisting of
 165 a collection of paleopoles whereby relevant parameters such as age, age uncertainty range, number of
 166 sites and the Fisher (1953) precision parameter K are provided. This allows the determination of the
 167 reference pole position and its B_{95} following the procedures described above. Alternatively, the user
 168 may also compute the RPDs relative to the geographic pole. The estimated vertical-axis rotation for
 169 each observed paleopole then simply corresponds to the absolute paleomagnetic declination at the
 170 chosen reference location based on that paleopole (Figs. 5a, b). The relative paleolatitudinal
 171 displacement corresponds to the absolute difference between the observed paleolatitude and the
 172 present-day latitude of the reference location. Because the position of the geographic pole has no
 173 uncertainty, the uncertainty of these results is determined by the A_{95} of the observed pole.

174 We quantify the relative paleomagnetic displacements as relative rotation (R) and latitudinal
 175 displacement (L) based on the difference in pole position between an observed paleopole and
 176 reference pole, calculated using a spherical triangle (Fig. 2). The rotation R (following the
 177 nomenclature of, for instance, Beck (1980) and Demarest (1983)) and is quantified by the angle
 178 between the great-circle segments that connect the sampling location with both paleopoles, which is
 179 identical to the difference between the paleomagnetic declinations predicted by the poles at the
 180 sampling location. To determine whether the rotation is clockwise or counterclockwise needs to be
 181 inferred from these declination values, as the angle in rotation space does not contain this information
 182 (see Butler (1992) for more detail). The paleolatitudinal displacement (L) is then determined by the
 183 difference between the angular distances p_{ref} and p_{obs} (i.e., the paleomagnetic colatitude of both poles)
 184 of the two great-circle segments, where $L = p_{ref} - p_{obs}$. A positive displacement value thus indicates
 185 that the paleomagnetic latitude of the observed pole is larger than that of the reference pole. Please
 186 note that L has the opposite sign of the poleward transport (P) defined by Butler (1992), whereby a
 187 positive value indicates a northward motion toward the reference pole, corresponding instead to a
 188 lower paleolatitude of the observed pole than predicted by the reference pole. We found the resulting
 189 plots counterintuitive, and therefore plot a more northerly (southerly) paleolatitude than expected
 190 from the reference pole position above (below) the 0° reference line (Fig. 7), following e.g., Kent and
 191 Irving (2010, their Figure 8). To quantify the uncertainties on relative paleomagnetic displacements,
 192 we follow the square-root formulas developed by Demarest (1983) and defined by Butler (1992) for
 193 a pole-space approach (see equations A.66 and A.76 in the Appendix), whereby the 95% confidence
 194 region on the reference pole ($A_{95, ref}$) is replaced by the B_{95} .

195

196 **2.3. Input and output**

197 The input for the APWP and RPD tools should be provided through the template file that can be
198 downloaded from the website ('Download the example input file'). This comma-separated values
199 (CSV) file consists of a header with column names under which the relevant data and metadata should
200 be added. Each entry that is included in the input file should contain the following parameters: the age
201 and age uncertainty range of the sampled rocks, the longitude and latitude of the mean sampling
202 location, the longitude and latitude of the paleopole, the number of paleomagnetic sites (N , i.e., the
203 number of spot readings of the paleomagnetic field), the Fisher (1953) precision parameter (K) and
204 the 95% cone of confidence about the pole (A_{95}). For the global APWP of Vaes et al. (2023), we only
205 used sediment-derived paleopoles that were corrected for inclination shallowing using the
206 elongation-inclination (E/I) correction of Tauxe and Kent (2004) and that satisfied the criteria
207 proposed by Vaes et al. (2021). This avoided the variable bias posed by potential inclination
208 shallowing and allows propagating the uncertainty associated with the E/I correction in the
209 calculation of the APWP (following the approach of Pierce et al. (2022); see section 3 in Vaes et al.
210 (2023) for more details). The input file thus includes an optional column for the uncertainty of the E/I
211 correction. This source of uncertainty can be accounted for in the computation of a custom APWP by
212 adding the mean difference between the shallowing-corrected paleolatitude estimate and the
213 associated 95% confidence limits.

214 The output of the APWP tool consists of a plot of the APWP on a northern hemisphere map
215 projection. The age and relevant parameters of each reference pole of the APWP is easily inspected by
216 hovering the mouse over the path. The custom APWP may be visually compared to the global APWP
217 of Vaes et al. (2023) – in the reference frame of a chosen plate – by adding a reference APWP to the
218 map using the 'Add reference APWP' button. The output APWP may be directly downloaded from the
219 web interface as a CSV file that contains the longitude and latitude values of the APWP, the center age
220 of the window, the mean age and number of the re-sampled VGPs for each time window, as well as the
221 P_{95} values and all other relevant statistical parameters. The custom APWP may be used directly in the
222 RPD portal to determine the relative paleomagnetic displacements between the studied tectonic plate
223 or terrane and a chosen reference plate (see examples in section 4).

224 For the computation of the RPDs in the RPD tool, the user may specify a few input parameters,
225 similar to the APWP tool. The number of iterations and time window (default is 10 Ma) used to
226 compute the reference pole position and its uncertainty (the B_{95}) can be provided as direct input on-
227 screen. Instead of using the sampling location of each entry in the input file, a reference location may
228 instead be chosen by the user to compute the RPDs (Fig. 4). Note that specifying a reference location
229 is required when using a custom APWP as input for this tool. As described in the previous section, the
230 user may choose the reference against which the uploaded input data are compared. The output of the
231 RPD tool consists of two figures on the web interface that show the relative vertical-axis rotations and
232 paleolatitudinal displacement computed for each input paleopole, which can be downloaded as raster

233 (PNG) or vector (SVG) image. As for the APWP tool, the output results may also be downloaded as a
234 CSV file.

235

236 **3. Reference database portal**

237 The final portal of APWP-Online.org hosts the reference database that underpins the global APWP for
238 the last 320 Ma from Vaes et al. (2023). Through this web interface (Fig. 8), the most recent version of
239 the global APWP – in the coordinate frame of all major tectonic plates – may be accessed and
240 downloaded, as well as the paleomagnetic database and the global plate circuit, which underlie the
241 computation of the APWP. This portal provides a platform where future updates of the global APWP
242 will be made available. We refer the reader to Vaes et al. (2023) for a detailed description of the
243 methodology and plate circuit. Any future updates of the APWP will be described in a change log on
244 the website and indicated with a version number (see Fig. 8), and any major future updates will be
245 accompanied by a peer-reviewed publication.

246 We intend to update the paleomagnetic database that underlies the computation of the global
247 APWP on an annual basis. The database is intended as a community effort, and a steering committee
248 of specialists will be maintained that will meet on an annual basis to evaluate new entries (see APWP-
249 online.org for the latest composition of the committee). Moreover, the database will be coupled to the
250 MagIC database (Jarboe et al., 2012).

251 We encourage researchers to submit new datasets that may contribute to the improvement of
252 the database. First, we welcome any new, high-quality paleomagnetic data obtained from stable plate
253 interiors – after publication in a peer-reviewed journal – that may be included in the database. New
254 data will be reviewed and against the reliability criteria described in Vaes et al. (2023). For
255 sedimentary data, these criteria require that the collection of paleomagnetic directions is corrected
256 for potential inclination shallowing (see e.g., Paleomagnetism.org (Koymans et al., 2016; 2020).
257 Inclusion of sediment-based data will be evaluated using the quality criteria proposed by Vaes et al.
258 (2021).

259 Second, we also welcome new age data that provides better constraints on the rock and/or
260 magnetization age of the paleomagnetic data that is included in the database. Any suggestions for
261 updating the age of specific paleopoles are highly appreciated and may be submitted through the
262 query form. We note that many of the age uncertainty ranges quoted in the current database
263 correspond to available age constraints at the time of the original publication of the paleomagnetic
264 data. Therefore, useful age data may also be provided by peer-reviewed articles that were already
265 published before the database of Vaes et al. (2023) was compiled. Finally, we welcome any corrections
266 to mistakes in our database, as well as new insights or doubts related to the reliability of certain
267 paleomagnetic datasets.

268

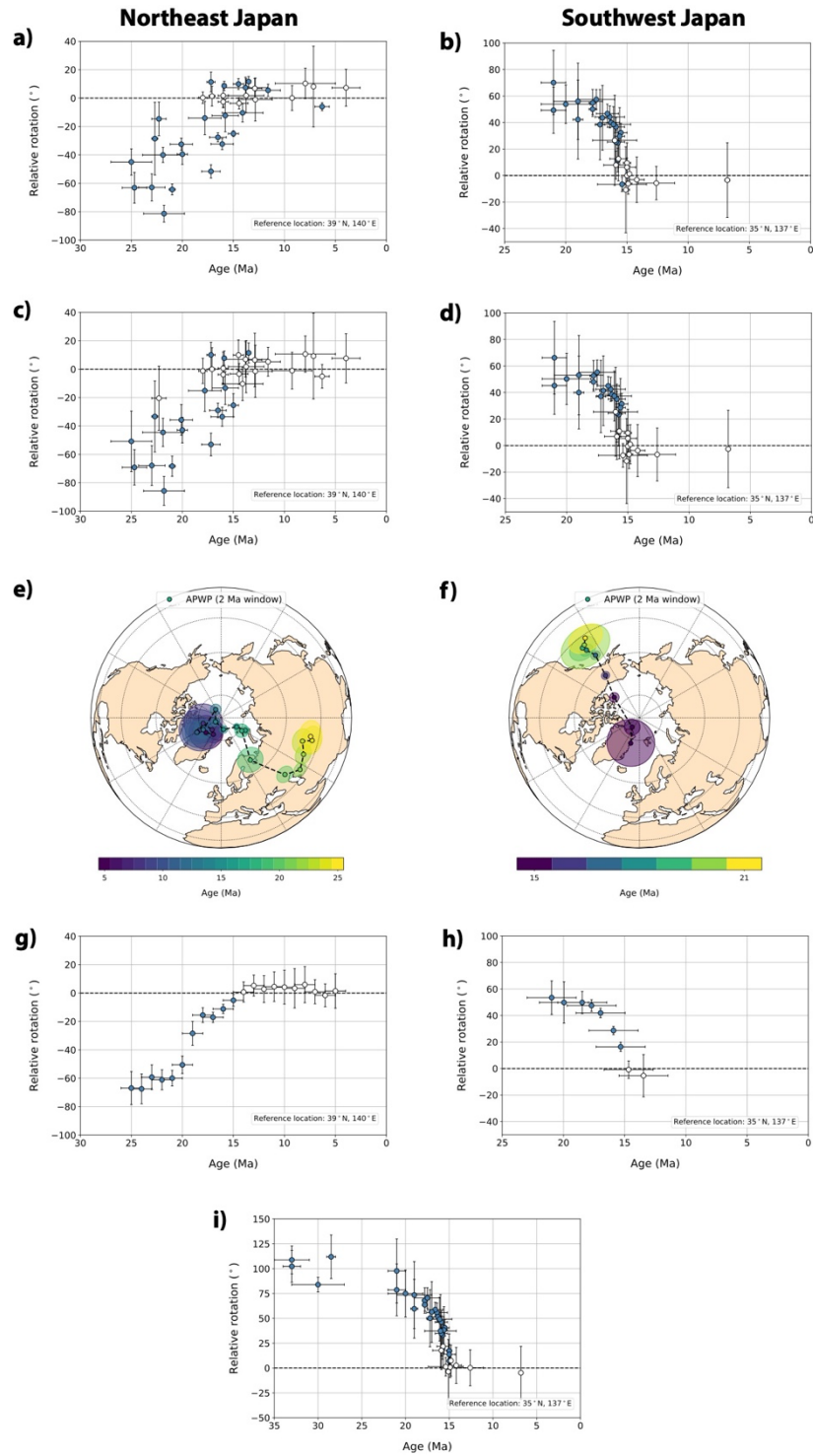


Fig. 5. Application of the APWP and RPD tools to the northeast and southwest Japan blocks. Vertical-axis rotations of each dataset relative to the geographic pole are shown in (a) and (b). A positive value indicates a clockwise rotation since that time. Rotations relative to Eurasia – using the global APWP of Vaes et al. (2023) – are shown in (c) and (d). Custom APWPs computed with the APWP tool, using a time window of 2 Ma and a temporal resolution of 1 Ma, are shown on orthographic plots in (e) and (f). Vertical-axis rotations relative to Eurasia are computed using these APWPs in (g) and (h). Finally, the rotation through time of southwest Japan relative to northeast Japan is shown in (i).

270 **4. Application to case studies**

271 We illustrate the functionalities of the two main tools of the APWP-online.org application by applying
272 them to two different case studies: the opening of the Japan Sea and the paleolatitudinal motion of the
273 intra-oceanic Olyutorsky arc (Figs. 5-7). We revisit the paleomagnetic data analyses performed by
274 Vaes et al. (2019) that was used to test their plate-kinematic reconstruction of the northwest Pacific
275 region. Vaes et al. (2019) reconstructed the motions of tectonic blocks relative to major plates (e.g.,
276 Pacific, North America, or Eurasia) based on marine magnetic and structural geological data, and by
277 placing their reconstruction in a paleomagnetic reference frame (of Torsvik et al., 2012), they
278 predicted the declination and paleolatitude for these tectonic blocks through time, at 10 Ma intervals.
279 They then compared the predicted declinations or paleolatitudes against paleomagnetic data from
280 these tectonic blocks and adjusted the reconstruction where required by paleomagnetic data and
281 permitted by structural data (see also Li et al., 2017 for procedures). Rather than comparing such
282 predictions against observed data, we show here how the APWP and RPD tools may be used to directly
283 quantify the magnitude, timing, and uncertainty of vertical-axis rotations and paleolatitudinal motions
284 relative to a chosen reference.

285 The opening of the Sea of Japan since ~25 Ma is well-known to have led to opposite rotations
286 of the northeastern and southwestern parts of Japan (e.g., Otofujii et al., 1985; Martin, 2011), and an
287 extensive paleomagnetic database has been collected over the years (Vaes et al., 2019). Using the RPD
288 tool, we may plot the individual study-mean poles compiled by Vaes et al. (2019) relative to the north
289 geographic pole (i.e., only the declination and the associated uncertainty are shown) (Fig. 5a, b). Next,
290 we may plot these data relative to the global APWP of Vaes et al. (2023) in the coordinates of Eurasia,
291 because these are the values that are relevant for kinematic restoration of the opening of the Japan
292 Sea (Fig. 5c, d). The difference between Figs. 5a-b and 5c-d are minor as Eurasia did not rotate much
293 relative to the north pole in the last 25 Ma, but the confidence regions are slightly larger in Fig. 5c-d
294 as the uncertainty in the position of the reference pole contributes to the overall uncertainty. While
295 the general amount and timing of the coherent rotation of northeast Japan is easily estimated from
296 these plots, the dispersion of the study-mean poles is large, owing to the limited number (<10) of
297 paleomagnetic directions underpinning many of these study-mean poles (Vaes et al., 2022; Gerritsen
298 et al., 2022) and, potentially, to minor differential rotations of smaller blocks (Yamaji et al., 1999).

299 To obtain a better estimate of the magnitude and timing of the counterclockwise rotation, we
300 constructed an APWP for the Japan blocks using the APWP tool: for the period of 25 to 5 Ma for
301 northeast Japan and of 21 to 13 Ma for southwest Japan. The underlying database is identical as the
302 one used for the plots of Figs. 5a-d. The high data density allows the computation of the APWP using
303 a time step of only 1 Ma and a sliding window of 2 Ma. This is a much higher temporal resolution than
304 typically used in the construction of (global) APWPs, which often have a resolution of 10 Ma (e.g.,
305 Besse & Courtillot, 2002; Torsvik et al., 2008, 2012; Vaes et al., 2023). For the northeast Japan block,
306 The APWP shows a phase of rapid polar wander between ~20 and 15 Ma followed by a stillstand of

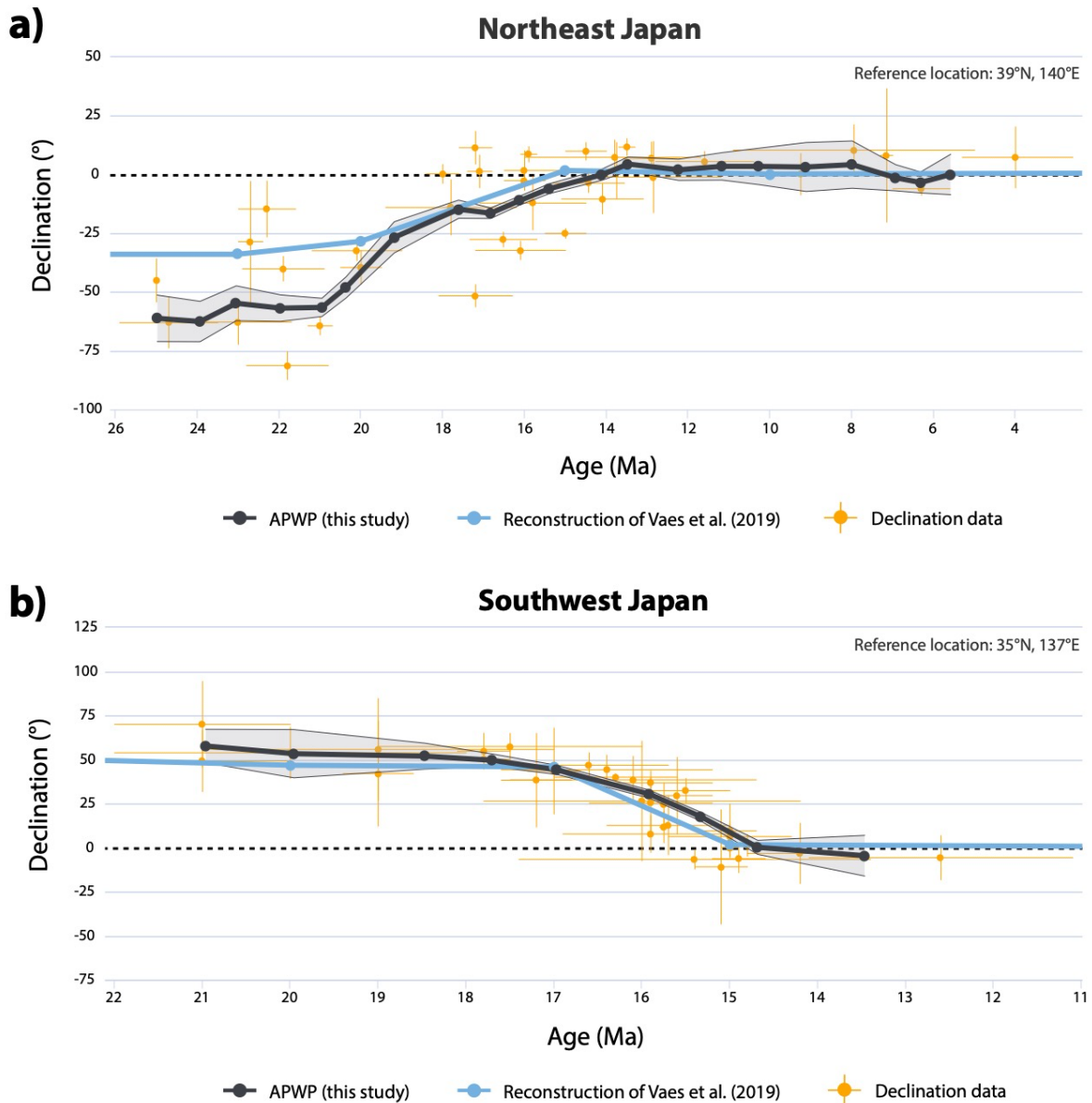


Fig. 6. Comparison of the declination curves predicted for northeast Japan (a) and southwest Japan (b) for a chosen reference location using the APWPs computed in this study (Figs. 5e, f) and using the plate-kinematic reconstruction of Vaes et al. (2019).

307 the paleomagnetic pole position after ~14 Ma (Fig. 5e). Likewise, southwest Japan reveals a rapid
 308 phase of polar wander between ~21-13 Ma, but data density before and after is insufficient for a
 309 meaningful APWP calculation (Fig. 5f). We assess whether these polar wander phases indeed
 310 correspond to a relative rotation by using the custom APWPs as input in the RPD tool and compute
 311 the vertical-axis rotation through time relative to Eurasia, which tightly constrains the timing and
 312 amount of the vertical-axis rotation phases (Fig. 5g, h). For illustration, we also compared the
 313 compilation of study-mean paleopoles from southwest Japan to the database of northeast Japan, by
 314 adding the latter as a 'custom reference database' in the RPD tool (Fig. 5i). The results reveal a relative
 315 rotation of ~100° during the opening of the Sea of Japan until ~15 Ma. Finally, we uploaded the new

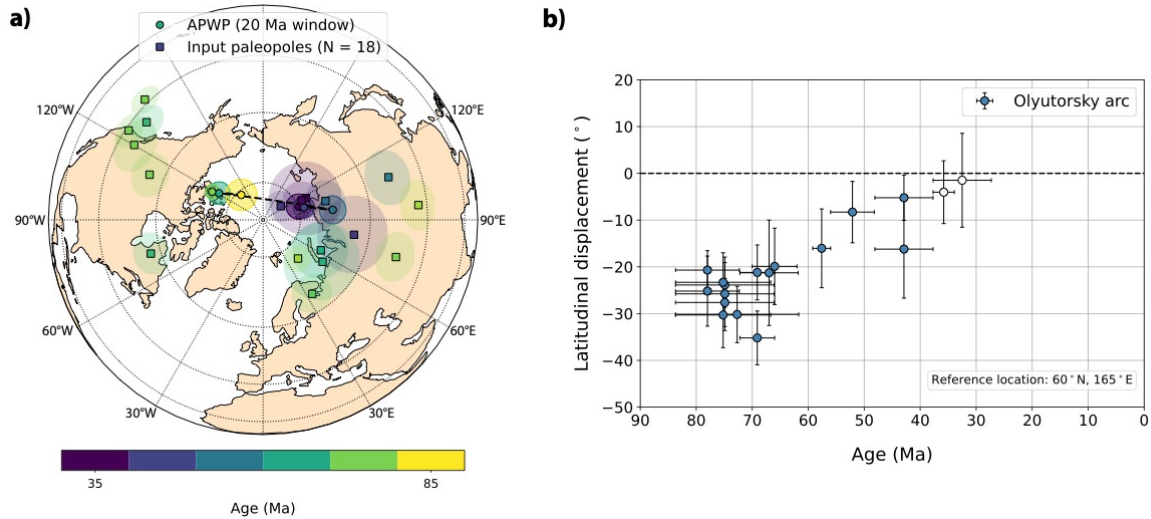


Fig. 7. Custom APWP computed for the data compilation of the Olyutorsky arc (a). Latitudinal displacement against age, relative to the North American plate.

316 APWPs for northeast and southwest Japan in the Geography Portal of Paleomagnetism.org 2.0
 317 (Koymans et al., 2020) to show how the declination values predicted by these APWPs compare to the
 318 declination curves predicted from the plate reconstruction of Vaes et al. (2019) (Fig. 6). The main
 319 difference between the curves obtained by Vaes et al. (2019) and those presented here is that the
 320 latter are purely based on paleomagnetic data and are computed at a much finer temporal resolution,
 321 providing tight paleomagnetic constraints on the rotation history of the Japanese islands during the
 322 Miocene opening of the Japan Sea.

323 We illustrate the application of the paleolatitudinal displacement (L) tool using a case study of
 324 the Olyutorsky arc (Fig. 7). The Olyutorsky arc is an extensive intra-oceanic arc complex that was
 325 emplaced onto continental crust of Kamchatka in the Eocene (~55-45 Ma, Vaes et al., 2019).
 326 Paleomagnetic data reveal that the arc was located far south of its present-day location (e.g.,
 327 Kovalenko, 1996; Levashova et al., 1997, 1998, Konstantinovskaya, 2001; Shapiro and Soloviev, 2009;
 328 Domeier et al., 2017; Vaes et al., 2019). In Fig. 7a, we show the relative paleolatitudinal displacement
 329 relative to the stable North American plate (of which the Kamchatka peninsula is currently part). In
 330 this case, computing an APWP for Olyutorsky is not meaningful, because sediment-derived datasets
 331 that have not been corrected for inclination shallowing and datasets have been strongly rotated
 332 relative to each other (see strongly scattered poles in Fig. 7b). Nonetheless, the data reveal a
 333 systematic decrease in the paleolatitude relative to North America of ~20-30° between the onset of
 334 arc magmatism around ~85-80 Ma and the obduction age of ~50 Ma (Fig. 7a), which is more
 335 informative for plate kinematic reconstruction purposes than the absolute paleolatitudes of the study-
 336 mean poles and the global APWP in North American coordinates that was used by Vaes et al. (2019).

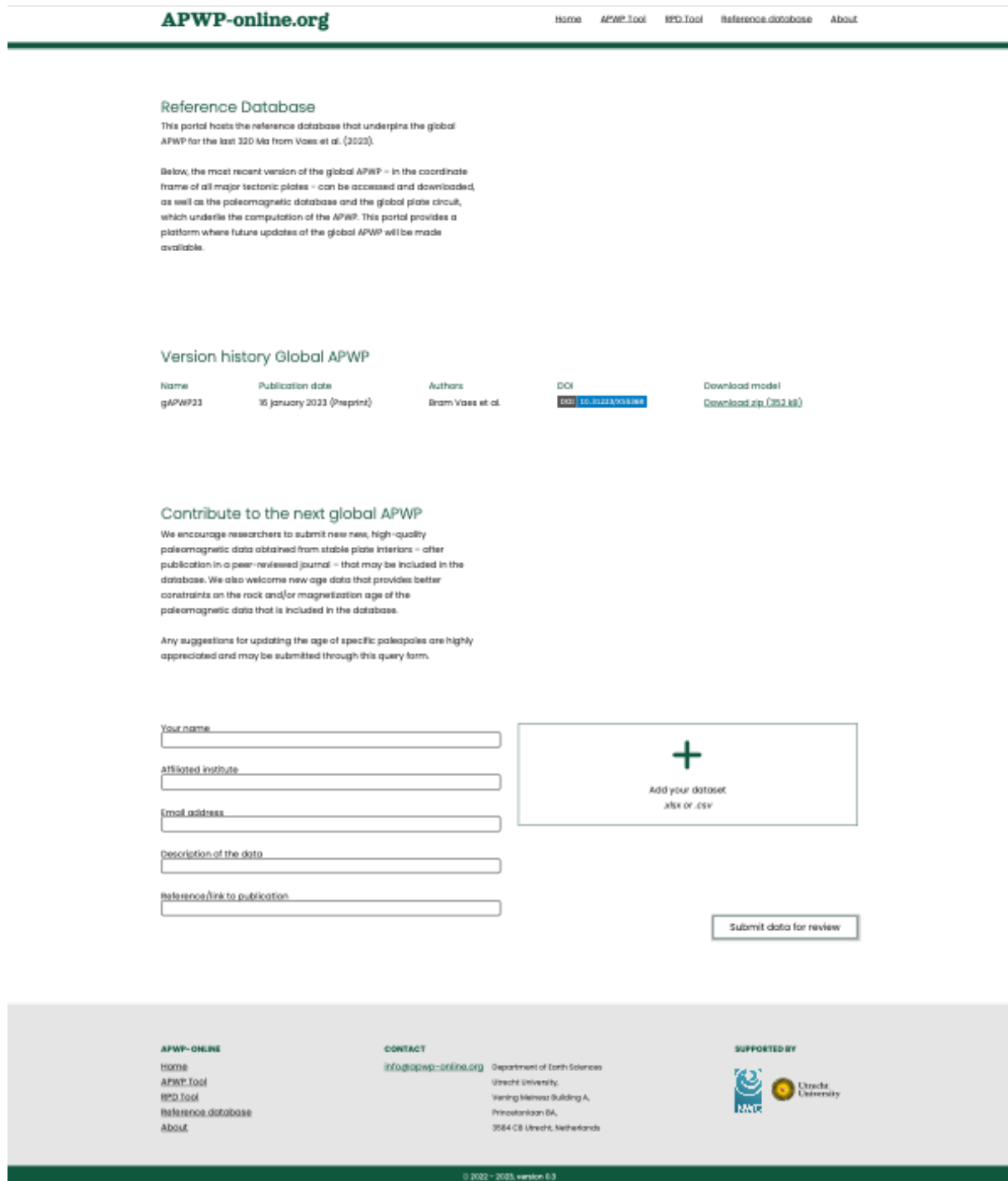


Fig. 8. Overview of the ‘Reference database’ portal.

337

338 **5. Availability, data storage and license**

339 The APWP-online.org application (<https://apwp-online.org>) can be freely accessed with the latest
340 versions of commonly used internet browsers, such as Google Chrome, Mozilla Firefox, and Safari. The
341 source codes of the web applications and the Python scripts that are used to perform the calculations
342 will be made publicly available on Github and archived on Zenodo upon acceptance of the manuscript.

343 All processing of paleomagnetic data and calculations are performed locally on the machine of the
344 user. No imported data or results are stored externally on a server or sent over the internet, ensuring
345 the integrity of the data and user. The input data and results are instead stored locally within the local
346 storage of the browser, and thus allow the user to continue using the webtools offline. The local
347 storage may also be downloaded by pressing the 'Download session' button, enabling users to
348 continue working with the input data and results at any later moment by re-uploading this file. In
349 addition, the local storage file may be shared among colleagues or added as a supplementary file to a
350 paper to facilitate evaluation and reproducibility of the analyses by peers. APWP-online.org is an
351 open-source web application licensed under the GNU General Public License v3.0.

352

353 **6. Conclusions**

354 APWP-online.org is an online, open-source application that enables paleomagnetists to compute
355 custom apparent polar wander paths and relative paleomagnetic displacements (RPD) using a
356 statistical approach that was recently developed by Vaes et al. (2022, 2023). The application consists
357 of three different portals: the APWP portal, the RPD portal and the Reference Database portal. The
358 APWP portal enables researchers to compute a custom APWP from site-level paleomagnetic from a
359 collection of paleopoles, using a chosen temporal resolution. The resulting APWP can then be
360 compared to a reference APWP using the RPD tool to determine the relative paleomagnetic
361 displacements through time. The RPD tools allow the identification and quantification of vertical-axis
362 rotations and paleolatitudinal displacements relative to a chosen APWP or pole, in which temporal
363 and spatial uncertainties are propagated and in which the uncertainty of the reference pole is
364 weighted against the number of paleomagnetic sites used to compute the studied paleomagnetic
365 direction or paleopole. Finally, the Global Database portal provides an up-to-date version of the global
366 APWP for the last 320 Ma in the coordinate frame of all major plates, as well as the paleomagnetic
367 database and plate circuit that underlie its computation. We invite paleomagnetists to submit new,
368 high-quality paleomagnetic data, or recommend modification of the existing database (e.g., the
369 revision of age constraints) through the query form included in this portal, such that the global APWP
370 can be regularly updated in the future. An international steering committee will update the database
371 and the global APWP behind APWP-online.org on an annual basis. We foresee that the accessible and
372 easy-to-use tools of APWP-online.org will enable specialist users to apply state-of-the-art methods for
373 computing apparent polar wander paths and tectonic displacements, which may contribute to solving
374 detailed tectonic or paleogeographic problems.

375

376 **Acknowledgements**

377 This study was funded by NWO Vici grant 865.17.001 to DJJvH. We thank Lydian Boschman for
378 discussion.

379

380 **Author contributions**

381 **BV**: conceptualization of study, data compilation and analyses, development of codes, figure drafting
382 and paper writing. **DJJvH**: conceptualization of study, paper writing and reviewing. **JP**: development
383 of web application, development of codes, paper reviewing.

384

385 **Data availability**

386 No new paleomagnetic data were used in this study. The paleomagnetic datasets used to illustrate the
387 applications of the tools were previously compiled by Vaes et al. (2019) and the original sources are
388 cited in the text of the current paper. We refer the reader to Vaes et al. (2019) for more details.

389

390 **References**

- 391 Beck Jr, M. E. (1980). Paleomagnetic record of plate-margin tectonic processes along the western edge
392 of North America. *Journal of Geophysical Research: Solid Earth*, 85(B12), 7115-7131.
- 393 Besse, J., and Courtillot, V. (2002). Apparent and true polar wander and the geometry of the
394 geomagnetic field over the last 200 Myr. *Journal of Geophysical Research: Solid Earth*, 107(B11),
395 EPM-6.
- 396 Butler, R. F. (1992). *Paleomagnetism: magnetic domains to geologic terranes* (Vol. 319). Boston:
397 Blackwell Scientific Publications.
- 398 Coe, R. S., Globberman, B. R., Plumley, P. W., & Thrupp, G. A. (1985). Paleomagnetic results from Alaska
399 and their tectonic implications.
- 400 Demarest Jr, H. H. (1983). Error analysis for the determination of tectonic rotation from
401 paleomagnetic data. *Journal of Geophysical Research: Solid Earth*, 88(B5), 4321-4328.
- 402 Domeier, M., Shephard, G. E., Jakob, J., Gaina, C., Doubrovine, P. V., & Torsvik, T. H. (2017).
403 Intraoceanic subduction spanned the Pacific in the Late Cretaceous-Paleocene. *Sciences Advances*,
404 3. eaao2303.
- 405 Fisher, R. A. (1953). Dispersion on a sphere. *Proceedings of the Royal Society of London. Series A.*
406 *Mathematical and Physical Sciences*, 217(1130), 295-305.
- 407 Gerritsen, D., Vaes, B., & van Hinsbergen, D. J. (2022). Influence of data filters on the position and
408 precision of paleomagnetic poles: what is the optimal sampling strategy? *Geochemistry, Geophysics,*
409 *Geosystems*, 23(4), e2021GC010269.
- 410 Harrison, C. G. A., and Lindh, T. (1982). A polar wandering curve for North America during the
411 Mesozoic and Cenozoic. *Journal of Geophysical Research: Solid Earth*, 87(B3), 1903-1920.
- 412 Jarboe, N. A., Koppers, A. A., Tauxe, L., Minnett, R., and Constable, C. (2012). The online MagIC Database:
413 data archiving, compilation, and visualization for the geomagnetic, paleomagnetic and rock
414 magnetic communities. In *AGU Fall Meeting Abstracts* (Vol. 2012, pp. GP31A-1063).

- 415 Kent, D. V., and Irving, E. (2010). Influence of inclination error in sedimentary rocks on the Triassic
416 and Jurassic apparent pole wander path for North America and implications for Cordilleran
417 tectonics. *Journal of Geophysical Research: Solid Earth*, 115(B10).
- 418 Konstantinovskaya, E. (2001). Arc-continent collision and subduction reversal in the Cenozoic
419 evolution of the Northwest Pacific: An example from Kamchatka (NE Russia). *Tectonophysics*, 333,
420 75–94.
- 421 Kovalenko, D. (1996). Paleomagnetism and kinematics of the Central Olyutorsky Range, Koryak
422 Highland. *Geotectonics*, 30, 243.
- 423 Koymans, M. R., Langereis, C. G., Pastor-Galán, D., & van Hinsbergen, D. J. (2016). Paleomagnetism.org:
424 An online multi-platform open source environment for paleomagnetic data analysis.
- 425 Koymans, M. R., van Hinsbergen, D. J. J., Pastor-Galán, D., Vaes, B., & Langereis, C. G. (2020). Towards
426 FAIR paleomagnetic data management through Paleomagnetism.org 2.0. *Geochemistry, Geophysics,*
427 *Geosystems*, 21(2), e2019GC008838.
- 428 Levashova, N. M., Bazhenov, M. L., & Shapiro, M. N. (1997). Late Cretaceous paleomagnetism of the
429 East Ranges island arc complex, Kamchatka: Implications for terrane movements and kinematics
430 of the northwest Pacific. *Journal of Geophysical Research*, 102(B11).
- 431 Levashova, N. M., Shapiro, M. N., & Bazhenov, M. L. (1998). Late Cretaceous paleomagnetic data from
432 the Median Range of Kamchatka, Russia: Tectonic implications. *Earth and Planetary Science Letters*,
433 163(1–4), 235–246.
- 434 Li, S., Advokaat, E. L., van Hinsbergen, D. J., Koymans, M., Deng, C., & Zhu, R. (2017). Paleomagnetic
435 constraints on the Mesozoic-Cenozoic paleolatitudinal and rotational history of Indochina and
436 South China: Review and updated kinematic reconstruction. *Earth-Science Reviews*, 171, 58–77.
- 437 Martin, A. K. (2011). Double saloon door tectonics in the Japan Sea, Fossa magna, and the Japanese
438 Island arc. *Tectonophysics*, 498(1–4), 45–65.
- 439 Otofujii, Y. I., Matsuda, T., & Nohda, S. (1985). Opening mode of the Japan Sea inferred from the
440 paleomagnetism of the Japan Arc. *Nature*, 317(6038), 603–604.
- 441 Pierce, J., Zhang, Y., Hodgin, E. B., & Swanson-Hysell, N. L. (2022). Quantifying Inclination Shallowing
442 and Representing Flattening Uncertainty in Sedimentary Paleomagnetic Poles. *Geochemistry,*
443 *Geophysics, Geosystems*, 23(11), e2022GC010682.
- 444 Rowley, D. B. (2019). Comparing paleomagnetic study means with apparent wander paths: A case
445 study and paleomagnetic test of the Greater India versus Greater Indian Basin hypotheses.
446 *Tectonics*, 38(2), 722–740.
- 447 Shapiro, M. N., & Solov'ev, A. V. (2009). Formation of the Olyutorsky–Kamchatka foldbelt: A kinematic
448 model. *Russian Geology and Geophysics*, 50, 668–681.
- 449 Tauxe, L., & Kent, D. V. (2004). A simplified statistical model for the geomagnetic field and the
450 detection of shallow bias in paleomagnetic inclinations: was the ancient magnetic field dipolar?
451 *Geophysical Monograph Series*, 145, 101–155.

- 452 Torsvik, T. H., Müller, R. D., Van der Voo, R., Steinberger, B., and Gaina, C. (2008). Global plate motion
453 frames: toward a unified model. *Reviews of Geophysics*, 46(3).
- 454 Torsvik, T. H., Van der Voo, R., Preeden, U., Mac Niocaill, C., Steinberger, B., Doubrovine, P. V., et al.
455 (2012). Phanerozoic polar wander, paleogeography and dynamics. *Earth-Science Reviews*, 114(3-
456 4), 325-368.
- 457 Vaes, B., Gallo, L. C., & van Hinsbergen, D. J. (2022). On pole position: causes of dispersion of the
458 paleomagnetic poles behind apparent polar wander paths. *Journal of Geophysical Research: Solid
459 Earth*, 127(4), e2022JB023953.
- 460 Vaes, B., Li, S., Langereis, C. G., & van Hinsbergen, D. J. (2021). Reliability of paleomagnetic poles from
461 sedimentary rocks. *Geophysical Journal International*, 225(2), 1281-1303.
- 462 Vaes, B., van Hinsbergen, D. J. J., van de Lagemaat, S.H.A., van der Wiel, E., Lom, N. Advokaat, E. L., . . .
463 and Langereis, C.G. (2023). A global apparent polar wander path for the last 320 Ma calculated from
464 site-level paleomagnetic data. *EarthArXiv*, <https://doi.org/10.31223/X55368>.
- 465 Vaes, B., Van Hinsbergen, D. J., & Boschman, L. M. (2019). Reconstruction of subduction and back-arc
466 spreading in the NW Pacific and Aleutian Basin: Clues to causes of Cretaceous and Eocene plate
467 reorganizations. *Tectonics*, 38(4), 1367-1413.
- 468 Yamaji, A., Momose, H., & Torii, M. (1999). Paleomagnetic evidence for Miocene transtensional
469 deformations at the eastern margin of the Japan Sea. *Earth, planets and space*, 51(2), 81-92.